Rock and Soil Mechanics

Volume 42 | Issue 8 Article 7

12-16-2021

Study on prestress long-term loss of anchor cable considering coupled multiple factors

Zhong-ju FENG
School of Highway, Chang'an University, Xi'an, Shaanxi 710064, China

Guan JIANG
School of Highway, Chang'an University, Xi'an, Shaanxi 710064, China

Rui-xin ZHAO
School of Highway, Chang'an University, Xi'an, Shaanxi 710064, China

Hou-sheng LONG
Shandong Hi-speed Group, Jinan, Shandong 250014, China

See next page for additional authors

Custom Citation

FENG Zhong-ju, JIANG Guan, ZHAO Rui-xin, LONG Hou-sheng, WANG Zheng-bin, ZHANG Zheng-xu, . Study on prestress long-term loss of anchor cable considering coupled multiple factors[J]. Rock and Soil Mechanics, 2021, 42(8): 2215-2224.

Study on prestress long-term loss of anchor cable considering coupled multiple factors

Authors

Zhong-ju FENG, Guan JIANG, Rui-xin ZHAO, Hou-sheng LONG, Zheng-bin WANG, and Zheng-xu ZHANG

Rock and Soil Mechanics 2021 42(8): 2215−2224 ISSN 1000−7598
https: //doi.org/10.16285/j.rsm.2020.6506 rocksoilmech.researchcommons.org/journal

Study on prestress long-term loss of anchor cable considering coupled multiple factors

FENG Zhong-ju[1], JIANG Guan[1], ZHAO Rui-xin[1], LONG Hou-sheng[2], WANG Zheng-bin[1], ZHANG Zheng-xu[2]

1. School of Highway, Chang'an University, Xi'an, Shaanxi 710064, China

2. Shandong Hi-speed Group, Jinan, Shandong 250014, China

Abstract: In order to study the long-term loss law of anchorage force and the calculation method of prestress loss of anchorage force, a calculation method of the prestress loss of anchorage force was proposed to account for three factors. The proposed method is based on the generalized Hooke's law, relaxation rate time-history response equation and improved coupling constitutive model. It was adopted to calculate the theoretical loss value of the anchor cable prestress coupled with the internal sliding lock of the anchor plate, the stress relaxation of the cable body steel strand, and the rock mass creep, respectively. In order to verify the accuracy of the long-term loss calculation method, the anchor cable pull-out failure test was also carried out. By analyzing the transfer mechanism of the pull-out load, it was determined that the pull-out stage of the free section of the load-incremental displacement curve was the working load interval of the anchor cable. The median value of the working load interval was taken as the effectiveness force of the anchor cable, and the measured value of the long-term loss of prestress was also obtained. Results show that the prestress loss of the anchor cable is about 17.5%-27.5% during 20 years. The rock mass creep is the most significant factor affecting the long-term loss of the anchor cable. Besides, there is an error of about 4.2% between the calculated value of the three-factor loss calculation method and the measured value of prestress loss at site. This verifies the accuracy of the three-factor loss calculation method, and also shows that the three-factor calculation method of long-term prestress loss mentioned here meets accuracy requirements and is feasible.

Keywords: prestressed cable; prestress losses; field pull-out test; anchorage force; rock creep

1 Introduction

Anchor cable support produces a stress compression zone within its action range by applying prestress, which makes the anchored rock mass in a triaxial stress state, exerting an active protection function. So, the deformation of the rock mass is effectively controlled and the stability of the slope can be guaranteed[1–4]. However, the anchoring system is affected by construction technology, engineering geology and environmental factors. Hence, the anchorage force is difficult to maintain the value of initial locking force. And the anchorage force decreases with time, i.e., the loss of anchorage force. The loss of anchorage force directly affects the safety of the anchoring structure, and poses a great risk to the long-term stable operation of anchoring structure. Therefore, it is of great theoretical and practical significance to study the various factors and the specific value of anchorage force loss.

Up to now, a large number of studies have carried out on the anchoring force loss and the long-term performance of the anchor cable. Zhang et al.[5] studied the various factors and calculation methods of anchoring force loss. Li et al. [6] established a prestress prediction model considering various factors of anchorage force loss, which can be used to analyze the long-term stability of anchoring projects. Xie et al.[7] studied the characteristics of soil creep and anchoring force loss under seepage action. Wang et al. [8] studied the prestress loss of pile–anchor support structure in thick alluvial clay layer under soil creep.

In actual anchoring engineering, the loss of anchorage force was affected by many factors. Zhu et al.[9], Wang et al.[10], and Chen et al.[11] studied the coupling effect of anchorage force loss of prestressed anchor cable and creep of rock and soil mass. Wang et al.[12] and Xiao et al.[13] established the prestressed loss model considering the relaxation characteristic of anchor cable. All the above calculations were the coupling calculation of anchorage force considering a single factor, and there was a deviation between the model and the actual situation. However, at present, there are still few studies on the loss of anchorage force considering various factors comprehensively. In addition, for the anchorage structure without embedded measuring elements for anchor cable force during construction, there is a lack of effective research methods to verify the calculation of anchorage force loss.

In the analysis of the sensitive factors of anchorage force loss, the change process and law of anchorage force were investigated and a method of computing anchorage force loss was developed based on the three-factor method in this paper. Reconstruction and expansion project of Beijing–Shanghai Expressway was analyzed as a case. The theoretical value of anchorage force loss subjected to various factors was calculated by using the generalized Hooke's law, the time-history response equation of relaxation rate, and the improved Nishihara coupled constitutive model. The self-designed cable extension device was used to carry out the in-situ pull-out failure test on the existing anchor cable so as

Received: 10 October 2020 Revised: 13 March 2021
This work was supported by the National Key Research and Development Project (2018YFC1504801) and the National Natural Science Foundation of China (41272285).
First author: FENG Zhong-ju, male, born in 1965, PhD, Professor, doctoral supervisor, mainly engaged in teaching and research in geotechnical engineering. E-mail: ysf@gl.chd.edu.cn

to measure the value of anchorage force loss. Finally, the calculated loss value based on the three-factor method was compared with the measured value of anchorage force loss to verify the accuracy of the three-factor method for prestress loss.

2 Long-term loss of anchor cable prestress

If the operation period of the anchorage system is more than 24 months, this project belongs to a long-term anchorage project. For a long-term anchoring project, there are four factors that cause the cable force loss. ① After the prestressed anchor cable is pulled, the loss of the locking of anchorage force is caused by the locking of the anchor space gap due to the internal shrinkage of steel strand of cable body. ② The anchored rock mass creeps and even plastically deforms during the slope operation period, resulting in long-term loss of anchorage force. ③ The stress relaxation of the cable along the stress direction was restrained by the anchored rock and soil during the slope operation period, causing stress relaxation loss. ④ It is difficult to maintain the original design bearing capacity of prestressed anchor cable due to corrosion, rainfall infiltration, temperature change and freezing-thawing cycles under the action of surrounding corrosive medium, resulting in loss of anchor force. Therefore, it is of great significance to study the various factors that affect the loss of anchorage force and correctly assess the proportion of the loss of each factor, for an in-depth understanding of the long-term performance of the anchor cable support and the reasonable improvement of the anchoring design calculation theory.

2.1 Sliding-locking in the anchor plate

There are a lot of gaps between the anchors, clips and backing plates at the tension end, and these gaps become tight when the prestressed cable is pulled and locked by using post-tensioning method, which make the exposed length of the cable body shorten and slip, leading to the loss in anchorage force.

The loss of anchorage force σ_{l1} caused by sliding-locking in the anchor plate can be calculated by generalized Hooke's law

$$\sigma_{l1}=\frac{a}{l}E_{\mathrm{s}} \tag{1}$$

where a is the shrinkage displacement of the cable body; l is the total length between tension end and the anchorage end, i.e., the total length of the free section of the anchor cable plus the anchor section; and E_{s} is the elastic modulus of prestressed anchor cable.

2.2 Stress relaxation of steel strand

After the prestressed anchor cable is tensioned and locked, the plastic deformation of the prestressed cable increases, and the elastic deformation decreases when the temperature and total strain remain unchanged. The phenomenon that the stress slowly decreased with time is the stress relaxation of the anchor cable. Relaxation rate [14] (R) is used to study the anchorage force loss σ_{l2} under long-term load. R is caused by relaxation deformation of anchor cable. The relaxation rate is defined as

$$R=\frac{\sigma_0-\sigma_{\mathrm{t}}}{\sigma_0}\times 100\% \tag{2}$$

where R is the relaxation rate (%); σ_0 is the initial stress (MPa); and σ_{t} is the stress acting on the sample at time t (MPa).

Under the condition that the nominal diameter of the steel strand is 15.2 mm and the tensile strength is 1 860 MPa, the results of stress relaxation test are shown in Fig. 1.

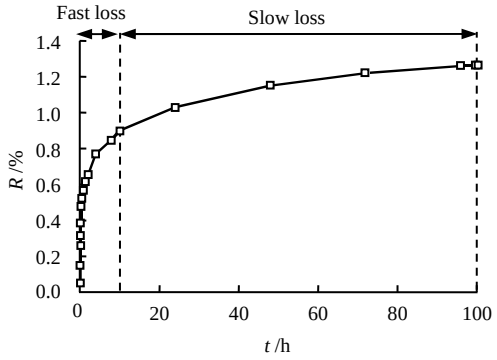

Fig. 1 Relationship between relaxation rate and time

It can be seen from Fig.1 that at the initial stage of anchorage force locking, the relaxation rate of the cable increases rapidly, and then enters the relaxation stable stage, the relaxation rate increases slowly and gradually stabilizes. In order to study the time-history sensitivity of the change of relaxation rate, the $\lg R-t$ relationship curve is plotted as shown in Fig. 2.

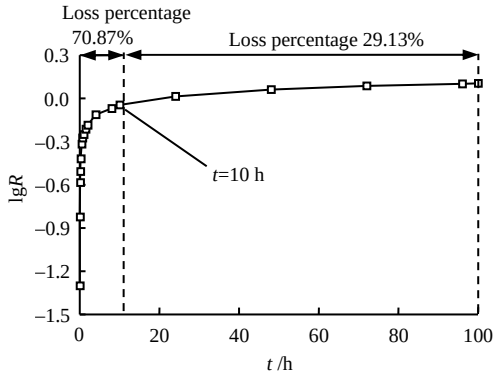

Fig. 2 Relationship between lg*R* and *t*

The relaxation loss of anchor cable accounts for 70.87% of the total relaxation at $t=10$ h during the whole test. At $t=24$ h, the relaxation loss of anchor cable completes 81.10% of the total relaxation during the whole test. After that, the relaxation rate starts to vary approximately smoothly. In order to obtain the time-history response equation of the relaxation rate, the $\lg R-\lg t$ relationship curve is drawn as shown in Fig. 3.

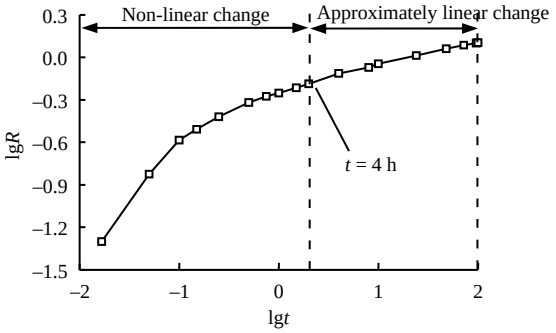

Fig. 3 Relationship between lg*R* and lg*t*

Figure 3 illustrates that in the initial stage, the $\lg R-\lg t$ relationship curve presents non-linear growth with a gradually decreasing growth rate. And in the final stage, $\lg R$ varies almost linearly with $\lg t$. An attempt can be made to establish the time-history response equation of the relaxation rate using the approximate straight line segment of the double logarithmic curve:

$$\lg Rt=\lg RT+k(\lg t-\lg T) \tag{3}$$

where T is the moment when the $\lg R-\lg t$ curve is transformed into a linear change; t is the total relaxation time history; $R(t)$ and $R(T)$ are the relaxation rates at the moments t and T; k is the slope of the approximate straight line segment of the $\lg R$ - $\lg t$ curve after moment T. Transforming Eq. (3) yields

$$R(t)=R(T)\left(\frac{t}{T}\right)^{k} \tag{4}$$

Taking into account the creep of the grouting cement and the anchored rock mass, the relaxation rate of the cable in the actual project is smaller than that measured from the field anchor cable test, so the original formula is multiplied by the reduction factor ξ:

$$R(t)=R(T)\xi\left(\frac{t}{T}\right)^{k} \tag{5}$$

Obviously, the relaxation loss of the anchor cable strand（σ_{l2}）is the product of the relaxation rate time-history response equation and the tension control stress (σ_{con}).

$$\sigma_{l2}=R(t)\sigma_{\mathrm{con}}=R(T)\xi\left(\frac{t}{T}\right)^{k}\sigma_{\mathrm{con}} \tag{6}$$

2.3 Creep coupling of rock and soil mass

The variation of the anchorage force of the supporting structure is closely related to the stress state and deformation of the rock mass [15]. When the supporting structure is pulled due to the creep of the rock mass, the anchorage force of the supporting structure has a tendency of increasing with time. When the supporting structure is compressed caused by the creep of the rock mass, the axial force of the supporting structure decreases with time. In the long-term operation of the slope, due to the time-dependent creep of the anchored rock mass, elastic compression and even plastic deformation would occur in the loaded area, and the supporting structure is in a state of compression, resulting in the loss of anchorage force of supporting structure.

The research shows that without considering the construction technology and construction quality, the prestress loss of the anchor cable caused by the creep of the anchored rock mass accounts for a large proportion of the total prestress loss of anchor cable. Currently, the calculation models for the long-term loss of anchorage force caused by the creep of rock mass during the slope operation period mainly include generalized Kelvin model, Burgers model, and Nishihara Rheological model [16–20]. The Nishihara rheological model (see Fig.4), a visco-elasto plastic model, can fully reflect the time-dependent creep characteristics of rock mass[21]. In Fig. 4, σ_{S} is the frictional resistance; E_{B} is the instantaneous modulus of elasticity; E_{K} is the hysteresis modulus of elasticity; η_{B} and η_{K} are the viscosity coefficients: η_{K} represents the creep rate in the initial creep stage, η_{K} characterizes the creep rate in the steady-state creep stage where the stress level is greater than the long-term strength.

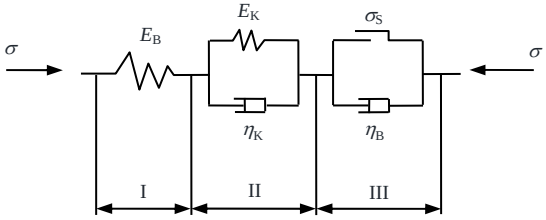

Fig. 4 Schematic diagram of Nishihara rheological model

In order to calculate the creep loss considering the coupling effect of the anchorage force, an improved Nishihara model was formed by paralleling the anchor cable element with the Nishihara model [22], which can be used to simulate the coordinated deformation of the anchored rock and the anchor cable, as shown in Fig. 5.

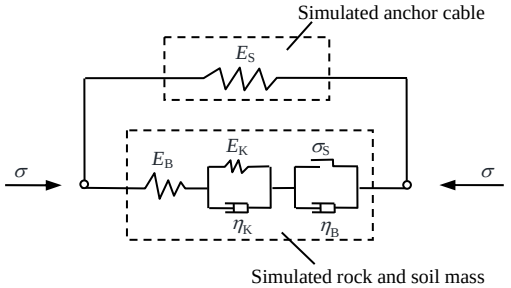

Fig. 5 Schematic diagram of the anchorage force coupled model

In Fig. 5, E_{S} is the equivalent elastic modulus of the prestressed anchor cable. Taking into account the coupling force of the anchor cable and the anchored rock mass, the elastic modulus of the anchor cable is equivalently transformed into:

$$E_{\mathrm{S}}=E_0\frac{A_{\mathrm{S}}}{A_{\mathrm{r}}} \tag{7}$$

where E_0 is the actual elastic modulus of the pre-stressed anchor cable; A_{S} is the area of prestressed anchor cable; and A_{r} is the area of the anchored rock mass with considering the coupling effect.

When $\sigma_0 \leqslant \sigma_{\mathrm{S}}$, in an ideal viscoplastic body, the friction plate can be regarded as a rigid body. Meanwhile, the mechanical properties of the Nishihara model are equivalent to the generalized Kelvin model and satisfy the following formula:

$$\sigma+\frac{\eta_{\mathrm{K}}}{E_{\mathrm{K}}+E_{\mathrm{B}}}\sigma'=\frac{E_{\mathrm{K}}E_{\mathrm{B}}}{E_{\mathrm{K}}+E_{\mathrm{B}}}\varepsilon+\frac{\eta_{\mathrm{K}}E_{\mathrm{B}}}{E_{\mathrm{K}}+E_{\mathrm{B}}}\varepsilon' \tag{8}$$

When the slope stress σ is a constant, Laplace transform is applied to Eq. (8) and the initial conditions ($t=0$, $\varepsilon=\dfrac{\sigma}{E_B}$) are substituted into the solution to obtain the creep equation of rock mass, as shown below:

$$\varepsilon=\frac{\sigma}{E_{\mathrm{B}}}+\frac{\sigma}{E_{\mathrm{K}}}\left(1-\mathrm{e}^{-\frac{E_{\mathrm{K}}}{\eta_{\mathrm{K}}}t}\right) \tag{9}$$

After the prestress is exerted by the tension anchor cable, when the anchored rock mass completes elastic deformation under the action of the initial strain ε_α applied by the anchor cable, the initial stress of the rock mass is σ_0 and the initial strain is ε_0. For the improved Nishihara model, there is

$$\varepsilon=\varepsilon_\alpha-\frac{\sigma}{E_{\mathrm{S}}} \tag{10}$$

By combining with anchorage coupling effect, we have

$$\left.\begin{aligned}\sigma_0&=E_{\mathrm{S}}\left(\varepsilon_\alpha-\varepsilon_0\right)\\ \sigma_0&=E_{\mathrm{B}}\varepsilon_0\end{aligned}\right\} \tag{11}$$

Solving the initial stress σ_0 of the rock mass, it can be obtained:

$$\sigma_0=\frac{E_{\mathrm{B}}E_{\mathrm{S}}\varepsilon_\alpha}{E_{\mathrm{B}}+E_{\mathrm{S}}} \tag{12}$$

Substituting Eq. (10) into Eq. (9), when the initial strain of the anchor cable is considered $\varepsilon_\alpha=\varepsilon_0$, it can be obtained:

$$\sigma=E_{\mathrm{S}}\varepsilon_\alpha-\frac{E_{\mathrm{S}}}{E_{\mathrm{B}}}\sigma_0-\frac{E_{\mathrm{S}}}{E_{\mathrm{K}}}\left(1-\mathrm{e}^{-\frac{E_{\mathrm{K}}}{\eta_{\mathrm{K}}}t}\right)\sigma_0 \tag{13}$$

The anchored coupling constitutive model is obtained as

$$\sigma=\frac{E_{\mathrm{B}}E_{\mathrm{S}}\varepsilon_\alpha}{E_{\mathrm{B}}+E_{\mathrm{S}}}-\frac{E_{\mathrm{B}}{E_{\mathrm{S}}}^2\varepsilon_\alpha}{E_{\mathrm{K}}\left(E_{\mathrm{B}}+E_{\mathrm{S}}\right)}\left(1-\mathrm{e}^{-\frac{E_{\mathrm{K}}}{\eta_{\mathrm{K}}}t}\right) \tag{14}$$

When $\sigma_0 \geqslant \sigma_{\mathrm{S}}$, the improved visco-elasto plastic model is equivalent to the Burgers model in which the frictional resistance σ_{S} is deducted from the stress. In Eq. (9), based on the assumption of ideal visco-plastic deformation, when $\sigma_0 \geqslant \sigma_{\mathrm{S}}$, the creep equation of the rock mass is obtained as follows:

$$\varepsilon=\frac{\sigma_0}{E_{\mathrm{B}}}+\frac{\sigma_0}{E_{\mathrm{K}}}\left(1-\mathrm{e}^{-\frac{E_{\mathrm{K}}}{\eta_{\mathrm{K}}}t}\right)+\frac{\sigma_0-\sigma_{\mathrm{S}}}{\eta_{\mathrm{B}}}t \tag{15}$$

Combining Eq. (10) and Eq. (15), we can get

$$\sigma=E_{\mathrm{S}}\varepsilon_\alpha-\frac{E_{\mathrm{S}}}{E_{\mathrm{B}}}\sigma_0-\frac{E_{\mathrm{S}}}{E_{\mathrm{K}}}\left(1-\mathrm{e}^{-\frac{E_{\mathrm{K}}}{\eta_{\mathrm{K}}}t}\right)\sigma_0-\frac{E_{\mathrm{S}}\left(\sigma_0-\sigma_{\mathrm{S}}\right)}{\eta_{\mathrm{B}}}t \tag{16}$$

Substituting Eq.(12) into Eq.(16), we can achieve the anchored coupling constitutive model

$$\sigma=\frac{E_{\mathrm{B}}E_{\mathrm{S}}\varepsilon_\alpha}{E_{\mathrm{B}}+E_{\mathrm{S}}}-\frac{E_{\mathrm{B}}{E_{\mathrm{S}}}^2\varepsilon_\alpha}{E_{\mathrm{K}}\left(E_{\mathrm{B}}+E_{\mathrm{S}}\right)}\left(1-\mathrm{e}^{-\frac{E_{\mathrm{K}}}{\eta_{\mathrm{K}}}t}\right)-\frac{E_{\mathrm{S}}\left(\sigma_0-\sigma_{\mathrm{S}}\right)}{\eta_{\mathrm{B}}}t \tag{17}$$

The anchoring coupled constitutive model considering the coordinated deformation of the anchored rock mass and the anchor cable is then proposed as follows:

$$\left.\begin{aligned}\sigma&=\frac{E_{\mathrm{B}}E_{\mathrm{S}}\varepsilon_\alpha}{E_{\mathrm{B}}+E_{\mathrm{S}}}-\frac{E_{\mathrm{B}}{E_{\mathrm{S}}}^2\varepsilon_\alpha}{E_{\mathrm{K}}\left(E_{\mathrm{B}}+E_{\mathrm{S}}\right)}\left(1-\mathrm{e}^{-\frac{E_{\mathrm{K}}}{\eta_{\mathrm{K}}}t}\right),\ \sigma_0\leqslant\sigma_{\mathrm{S}}\\ \sigma&=\frac{E_{\mathrm{B}}E_{\mathrm{S}}\varepsilon_\alpha}{E_{\mathrm{B}}+E_{\mathrm{S}}}-\frac{E_{\mathrm{B}}{E_{\mathrm{S}}}^2\varepsilon_\alpha}{E_{\mathrm{K}}\left(E_{\mathrm{B}}+E_{\mathrm{S}}\right)}\left(1-\mathrm{e}^{-\frac{E_{\mathrm{K}}}{\eta_{\mathrm{K}}}t}\right)-\frac{E_{\mathrm{S}}\left(\sigma_0-\sigma_{\mathrm{S}}\right)}{\eta_{\mathrm{B}}}t,\ \sigma_0\geqslant\sigma_{\mathrm{S}}\end{aligned}\right\} \tag{18}$$

Obviously, the creep loss σ_{l3} considering the coupling effect of anchorage force satisfies the following condition:

$$\sigma_{l3}=\sigma-\sigma_0 \tag{19}$$

Then, the creep loss σ_{l3} of the anchored rock mass can be obtained:

$$\left.\begin{aligned}\sigma_{l3}&=\frac{E_{\mathrm{B}}{E_{\mathrm{S}}}^2\varepsilon_\alpha}{E_{\mathrm{K}}\left(E_{\mathrm{B}}+E_{\mathrm{S}}\right)}\left(1-\mathrm{e}^{-\frac{E_{\mathrm{K}}}{\eta_{\mathrm{K}}}t}\right),\ \sigma_0\leqslant\sigma_{\mathrm{S}}\\ \sigma_{l3}&=\frac{E_{\mathrm{B}}{E_{\mathrm{S}}}^2\varepsilon_\alpha}{E_{\mathrm{K}}\left(E_{\mathrm{B}}+E_{\mathrm{S}}\right)}\left(1-\mathrm{e}^{-\frac{E_{\mathrm{K}}}{\eta_{\mathrm{K}}}t}\right)-\frac{E_{\mathrm{S}}\left(\sigma_0-\sigma_{\mathrm{S}}\right)}{\eta_{\mathrm{B}}}t,\ \sigma_0\geqslant\sigma_{\mathrm{S}}\end{aligned}\right\} \tag{20}$$

2.4 Influence of external factors on prestress loss

The three factors discussed above are the main factors causing the long-term loss of anchorage force, but there are still many factors such as anchor cable corrosion, rainfall, temperature. The anchor cable is rusted under the action of surrounding corrosive medium, which reduces the bonding strength of the anchor cable–grouting interface. In addition, the effective

bearing area of the steel strand reduces, which will cause damage to the anchoring performance. In the case of heavy rainfall on the slope, rainwater infiltrates and accumulates inside the slope, which increases the downward trend of the loose surface rock mass, generating additional anchorage force. But the additional anchorage force disappears after the fissure water dissipates, so the additional anchorage force is cyclically loaded. Under this action, the long-term strength of the steel strand is weakened. The change of temperature will also affect the anchoring performance, mainly because it can change the natural relaxation process of the steel strand of cable. In the meanwhile, corrosion of anchor cables, changes in rainfall and temperature can also cause loss of prestress. Since the influence of these factors on the anchoring performance is affected by site conditions and environmental factors, the results here are highly discrete. And these factors usually account for a small proportion of the total loss of anchorage force, so they are not considered in the long- term loss of anchorage force in this work.

2.5 Long-term loss of anchor cable prestress

Previous studies [23] have shown that after the anchor cable of the anchoring project was tensioned and locked, three-stage characteristics were presented in the time-history of the anchorage force, and they were rapid loss, slow loss, and stability loss, as shown in Fig. 6.

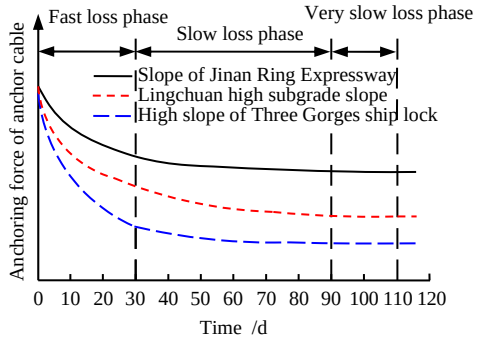

Fig. 6 Variation of the anchorage force with time

It can be seen from Fig. 6 that the anchorage force time-history curves of different anchoring projects are different. However, for these different anchoring projects, the three-stage characteristics of rapid loss, slow loss, and stability loss are roughly the same. The rapid loss stage generally occurred in 10 to 30 d, and the slow loss stage lasted for 50 to 80 d. The anchorage force generally entered stable loss stage after 90 d. Therefore, for an anchored slope with an operating period of more than 1 year, the initial calculation time history of anchorage force loss is recommended to be 90 days.

The existing research results[24–29] show that the loss caused by the sliding-locking in the anchor plate accounted for about 3%–9% of the initial locking value. The relaxation loss of long-term loaded steel strands usually accounted for 5%–10% of the initial locking value. The long-term creep loss of anchored rock mass accounted for about 5%–12% of the initial locking value, and the time-dependent behavior was the most obvious. The above three factors are the main factors that cause the loss of anchorage force. Combined with the influence factors of anchorage force loss, it is found that in the stage of rapid loss, the force loss stemmed from slippage locking of anchor pads and stress relaxation of cable strand. In the slow loss stage, the force loss was caused by the coupling creep between the anchored rock mass and the prestressed anchor cable. The influence of each factor on the anchorage force was relatively small or had been basically completed in the stable loss stage. Without considering the construction method and quality, a calculation method of prestress loss of anchor cable based on three factors was developed.

$$\sigma_l = \sigma_{l1} + \sigma_{l2} + \sigma_{l3} \tag{21}$$

where σ_l is the total loss of three-factor theoretical anchorage force.

3 Engineering application

The prestress loss in prestressed anchor cables installed in the K503+585–K504+018 left slope of the Beijing–Shanghai Expressway was analyzed as an example using the three-factor loss method proposed in this paper. The parameters were substituted into the Eq.(21) to compute the loss of anchorage force, and then the applicability of Eq.(21) was verified by the measured value obtained from in-situ pull-out failure test.

3.1 Project overview

The Laiwu–Linyi section of the Beijing–Shanghai Expressway was opened to traffic in November 2000, and it has been in operation for 20 years. The joints and fissures are developed in K503+585–K504+018 left slope. The lithology is mainly broken stone, strongly weathered limestone, and moderately weathered limestone. The geometry of the slope consists of five benches. The total height of the slope is 46.6 m and the slope angle is 1:0.5. The slope is supported by prestressed anchor cables. The supporting structure is a prestress cable with a spacing of 4 m and a length of 20 m. The designed pull-out capacity of a single anchor cable is 600 kN. The geological engineering profile of the slope is shown in Fig. 7. And the design parameters of prestressed anchor cable and the mechanical parameters of rock mass are listed in Tables 1 and 2.

3.2 Calculation example of long-term loss of prestress

3.2.1 Calculation for σ_{l1}

According to the attached table in *Specifacations for Design of Highway Reinforced Concrete and Prestressed Concrete Bridges and Culverts* (JTG 3362—2018) [30], it can be found that the clip-type anchor a is 4 mm. The total length of anchor cable is 20 m according to Table 1, that is, the distance between the

tension end and the anchorage end is 20 m. The elastic modulus of 1 860 MPa prestressed anchor cable is $E_0 = 1.95 \times 10^5$ N/mm2. Substituting these parameters into Eq. (1), we can get $\sigma_{l1} = 39.00$ N/mm^2.

3.2.2 Calculation for σ_{l2}

In the case that the nominal diameter of the steel strand is 15.2 mm and the tensile strength is 1 860 MPa, when $T = 4$ h, the curve of $\lg R - \lg t$ is converted to a linear trend, and the relaxation rate $R(T) = 0.77\%$. According to the aforementioned study on the anchorage force loss, the $\lg R - \lg t$ curve is close to a straight line with a slope of $k = 0.156$ and a reduction coefficient of $\xi = 0.8$ after moment T. According to *Technical Code for Engineering of Ground Anchor and Shotcrete Support* (GB50086–2015) [31], the tensile control stress is taken as $\sigma_{\text{con}} = 0.7 f_{\text{ptk}}$ where $f_{\text{ptk}} = 1\ 860$ MPa is the standard value of the cable tensile strength. According to the aforementioned analysis for the change process and law of anchorage force, the total relaxation time-history t is taken as the end of slow loss stage and the beginning of stable loss stage i.e., $t = 90$ d. Substituting $t = 90$ d into Eq.(6), we can get $\sigma_{l2} = 21.40$ N/mm^2.

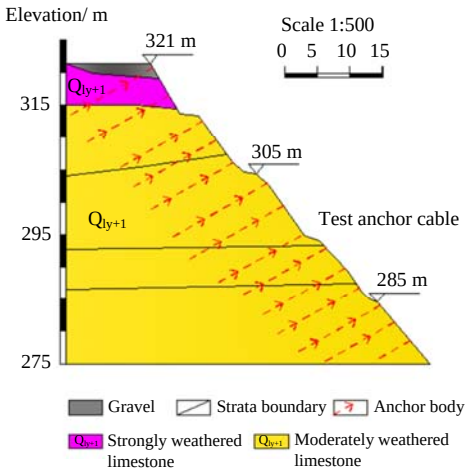

Fig. 7 Engineering geological profile of the high slope of the Beijing–Shanghai Freeway in K503+585–K504+018

Table 1 Design parameters of prestressed anchor cable

Free section length /m	Anchoring section length /m	Diameter	Inclination /(°)	Spacing /m	Tensile strength of steel strand /MPa	Design pull-out capacity /kN
16.5	3.5	5 bundles of steel stranded wires with a nominal diameter of 15.2 mm	30	Both longitudinal and transverse spacing are 4	1 860	600

Table 2 Parameters of slope rock mass materials

Material	Unit weight γ /(kN·m^{-3})	Cohesion c /kPa	Internal friction angle φ/(°)
Strongly weathered limestone	23.0	120	29
Moderately weathered limestone	23.6	260	55

3.2.3 Calculation for σ_{l3}

The rock mass of the K503+585–K504+018 left side slope in Beijing–Shanghai Expressway was sampled and the creep mechanics tests were carried out on the specimens. The load, corresponding to the sudden change in the displacement of the measured curve in the in-situ pull-out test, was used to back calculate the anchoring coupling model parameters [32]. Finally, the coupling calculation parameters of anchorage force of anchor cable in a three-bench slope were obtained, as shown in Table 3.

Table 3 Parameters of the anchorage force coupling model

E_{B} /MPa	E_{K} /MPa	η_{K} /(MPa·h^{-1})	η_{B} /(MPa·h^{-1})	E_{S} /MPa	A_{r} /mm^2	ε_α /mm
3 144	85	527 457	5 367 308	3 498	38 750	4.40×10^{-3}

In Table 3, the initial strain the anchor cable exerts is ε_α, which can be solved by the relationships between the initial strain and the initial prestress P_0 and the strain of rock mass ε_0.

$$\left.\begin{aligned} \varepsilon_\alpha &= \varepsilon_0 \\ P_0 &= E_S \varepsilon_0 A_r \end{aligned}\right\} \quad (22)$$

The initial prestress P_0 was taken as 600 kN according to the designed load, and all the parameters required were substituted into the solution, then we can obtain $\varepsilon_\alpha = 4.40 \times 10^{-3}$ mm.

According to the above research on the change process and law of anchorage force, the total coupled creep time-history was $t = 90$ d. Substituting $t = 90$ d into Eq. (20), we can obtain $\sigma_{l3} = 87.12$ N/mm^2。

Theoretical value of long-term loss of prestress of anchor cable installed in a three-bench slope is σ_l, $\sigma_l = \sigma_{l1} + \sigma_{l2} + \sigma_{l3} = 147.52$ N/mm^2.

The rock mass at the tested anchor cable position of the left slope from K503+585 to K504+018 of Beijing–Shanghai Expressway was sampled by the same method, and the anchorage force coupling model parameters were obtained. Theoretical loss of anchorage force in six tested anchor cables are listed in Table 4.

Table 4 Theoretical loss of anchorage force in tested anchor cable

Anchor cable number	MS-1	MS-2	MS-5	MS-3	MS-4	MS-6
Theoretical loss /(N·mm^{-2})	230.54	210.97	231.80	165.09	147.52	164.19

4 Verification

To further verify the accuracy of the calculation method for the long-term loss of anchorage force, the in-situ pull-out tests were carried out. By analyzing the test mechanism and load transfer mechanism, combining the load–displacement curve of the anchor cable, the time-dependent anchorage force is expect to obtain.

4.1 Test conditions

After the acceptance of the prestressed anchor

cable on site, the exposed length is too short to completely pass through the inner cavity of the jack. In order to accurately achieve the load–displacement curve of the prestressed anchor cable and avoid the loss of prestress of the anchor cable caused by the destruction of the anchor head, which can lead to the failure of reaching the research goal, an independently designed lengthening cable device[33] was adopted to conduct pull-out tests on the existing anchor cables after they were extended through the jack. The testing system schematic diagrams of the pull-out test are shown in Figs. 8 and 9, and the schematic diagram of the anchor cable length extension is shown in Fig. 10.

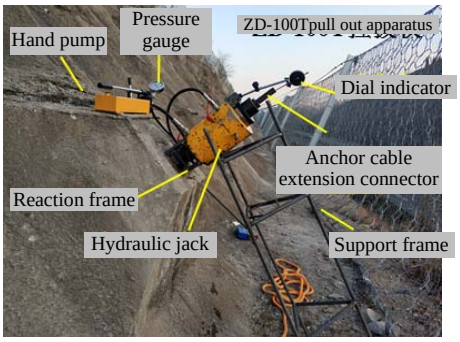

Fig. 8 ZD-100T anchor cable pull-out test system

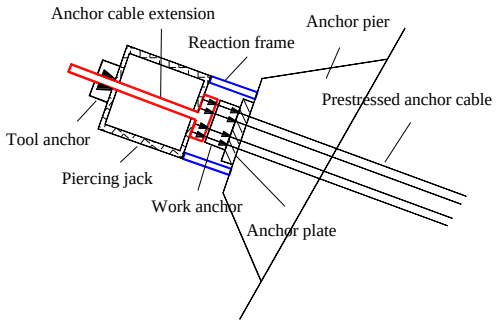

Fig. 9 Schematic diagram of the anchor cable pull-out system

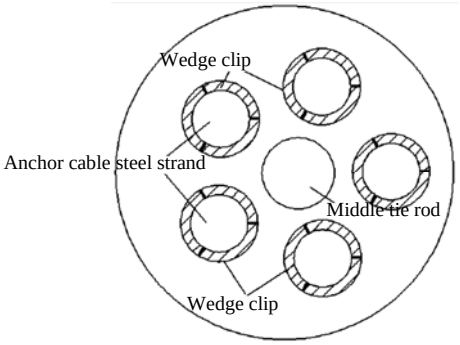

Fig. 10 Schematic diagram of lengthening cable device

In order to reduce the randomness of the test data and reflect the state of the anchorage force at different positions of the whole slope to the greatest extent, six test anchor cables were selected for in-situ pull-out failure test. These test anchor cables were located at the middle, the left and the right of the slope in the second and third benches of slope. The specific layout diagram is shown in Fig. 11.

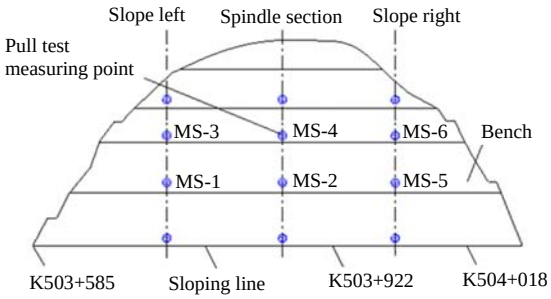

Fig. 11 Layout of tested prestressed anchor cables

4.2 Test results

According to the reading of dial indicator when the pull load was stable, the cumulative displacement of six cables (MS-1–MS-6) at different levels of pull loads were obtained. The displacement of three anchor cables (MS-1, MS-2, MS-5) in secondary bench slope increased significantly continuously when they were loaded to 630 kN. However, for the three anchor cables in third bench slope (MS-3, MS-4, MS-6), the increase of displacement was still not obvious. So, they were over-loaded to 750 kN, and the results are shown in Fig. 12.

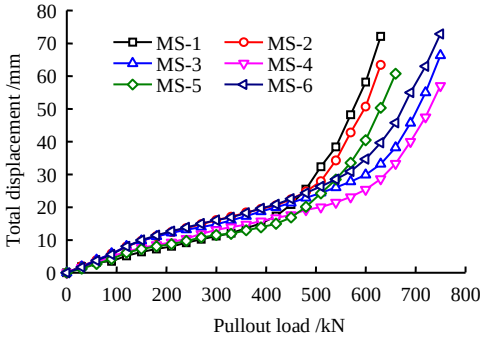

Fig. 12 Pull-out load–cumulative displacement curves of prestressed cable

It can be seen from Fig.12 that the cumulative displacement of each anchor cable shows a monotonous increasing trend with the increase of load, and the displacement increases sharply when the load reached 420–510 kN. However, the load–cumulative displacement curve of anchor cable can hardly reflect the displacement change of anchor cable under different loads sensitively. Therefore, the normal load–displacement increment curve of the anchor cables in secondary bench slope is shown in Fig.13, and the over load–displacement increment curve of the anchor cables in third bench slope is shown in Fig.14.

As observed from Figs. 13 and 14, the relationships between incremental displacement and load are nonlinear both under normal loading and over loading. Three characteristic points were taken, which were incremental displacement reduction point *A* and incremental displacement slow increase point *B*, and incremental displacement

steep increase point *C*. These three characteristic points divided the load–incremental displacement curve of the anchor cable into four stages, and then the summarized general law of the pull-out test on the prestressed anchor cable in this project is shown in Fig. 15.

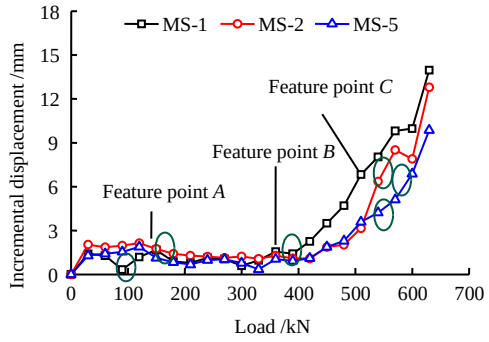

Feature point *A* (Incremental displacement decrease)
Feature point *B* (Incremental displacement increases slowly)
Feature point *C* (Incremental displacement increase dramatically)

Fig. 13 Load–displacement increment curves of prestressed cable in secondary bench slope

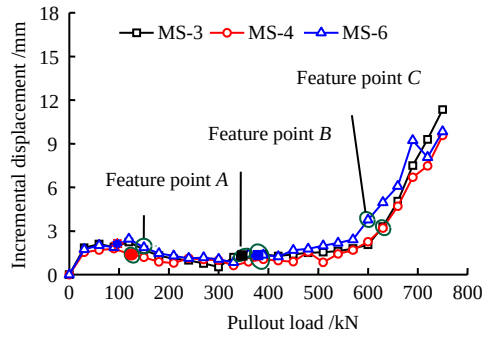

Feature point *A* (Incremental displacement decrease)
Feature point *B* (Incremental displacement increases slowly)
Feature point *C* (Incremental displacement increase dramatically)

Fig. 14 Pull-out load–displacement increment curves of prestressed cable in third bench slope

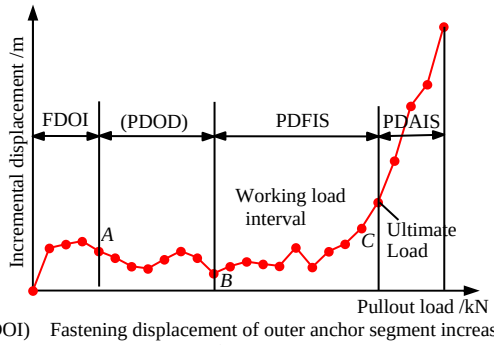

(FDOI) Fastening displacement of outer anchor segment increases
(PDOD) Pull displacement of outer anchor segment decreases
(PDFIS) Pull displacement of free section increases slowly
(PDAIS) Pull displacement of anchorage section increases sharply

Fig.15 Load–incremental displacement curve of prestressed cable

The incremental displacement curve of the anchor cable presents the variation characteristics of increasing–decreasing–slowly increasing–sharply increasing. The anchor cables go through four stages when they are subjected to the load of pulling, including outer anchor segment fastening, outer anchor segment tensioning, free section tensioning and anchoring section tensioning. The working load of the anchor cable is at the stage of free section tensioning. Before this stage, the free section of the prestressed cable is not fully tensioned. After this stage, the bonding force of the anchoring section cannot overcome the shear stress caused by tensioning. In the stage of free section tensioning, slipping and debonding occur between the anchor outer segment of prestressed cable and the concrete of pier, which resulted in force redistribution in anchor cable system, and the free section of the anchor cable begins to be stressed. This stage can be regarded as the stretching of the anchor cable of the free section under the action of linearly increasing load. The load at the beginning and end of the curve is the extreme value of the working load of the anchor cable. The time-dependent anchorage force is taken as the median value of its working load range. The time-dependent anchorage force and measured long-term loss values of 6 groups of anchor cables are shown in Tables 5 and 6.

Table 5 Time-dependent anchorage force of anchor cable on site

Anchor cable number	Feature point *B* /kN	Feature point *C* /kN	Workingload /kN	Time-dependent anchorage force /kN
MS-1	360	510	360–510	435
MS-2	360	540	360–540	450
MS-5	360	510	360–510	435
MS-3	330	630	330–630	480
MS-4	360	630	360–630	495
MS-6	360	600	360–600	480

Table 6 Long-term prestress loss of anchor cable measured on site

Anchor cable number	Time-dependent anchorage force /kN	Measured loss force /kN	Loss rate /%	Measured loss σ_c /(N·mm^{-2})
MS-1	435	165	27.5	235.71
MS-2	450	150	25.0	214.28
MS-5	435	165	27.5	235.71
MS-3	480	120	20.0	171.42
MS-4	495	105	17.5	150.00
MS-6	480	120	20.0	171.42

It can be seen from Tables 5 and 6 that the time-dependent anchorage force of six groups of tested anchor cables at different locations is 435–495 kN, and the prestress loss rate of anchor cable during 20 years of operation is 17.5%–27.5%. In order to verify the feasibility of the three-factor calculation method in the long-term prestress loss, the field measured prestress loss values were compared with the theoretical values of long-term prestress loss based on the three-factor method, as shown in Table 7.

It can be seen from Table 7 that the theoretical prestress loss value obtained from the three-factor method is slightly smaller than that the measured one on site. This is because, in this paper, the use of the three-factor method to obtain the theoretical values only considers the three main factors of long-term prestress loss, but the prestress loss is also affected by

other factors. The maximum error between the two is only 4.2%, which is within the acceptable range of the project and has certain feasibility.

Table 7 Comparison of theoretical values by the proposed method and measurements at site

Anchor cable number	Theoretical loss /(N·mm^{-2})	Measured loss σ_c /(N·mm^{-2})	Error /%
MS-1	230.54	235.71	2.2
MS-2	210.97	214.28	1.5
MS-5	231.80	235.71	1.7
MS-3	165.09	171.42	3.7
MS-4	147.52	150.00	1.6
MS-6	164.19	171.42	4.2

5 Conclusion

(1) The main factors affecting the long-term prestress loss of anchor cable are sliding-locking of anchor plate, stress relaxation of steel strand, and creep of anchored rock mass, among which the long-term prestress loss caused by the creep of anchored rock mass is the most significant. The long-term prestress loss of the anchor cable is $\sigma_l = \sigma_{l1} + \sigma_{l2} + \sigma_{l3}$.

(2) The pull-out test of anchor cable was divided into four stages: tightening of outer anchor section, tensioning of outer anchor section, tensioning of free section, and tensioning of anchor section. The tensioning stage of the anchoring section is the working load interval, and the median value of the working load interval is the time-dependent anchorage force of the anchor cable. The long-term loss of the prestressed anchor cable measured on site is from17.5% to 27.5% during the 20-year operation period.

(3) The error between the theoretically calculated value of long-term prestress loss of anchor cable based on the three-factor method and the measured value of long-term prestress loss of anchor cable on site is 4.2%, which meets the requirements of engineering accuracy and has certain feasibility.

References

[1] FENG Zhong-ju, ZHANG Yong-qing, LI Jin, et al. Study of displacement of bridge pier and abutment foundation caused by earth piling load and its prevention technique[J]. Journal of Highway and Transport, 2004(3): 77–80.

[2] FENG Zhong-ju, ZHANG Yong-qing. The inclination prevention of pier on the landslide by prestress anchor cable technique[J]. Journal of Xi'an Highway University, 2001(3): 39–41.

[3] FENG Zhong-ju, ZHU Yan-ming, GAO Xue-chi, et al. Safety evaluation model of excavating rock slope based on entropy-grey correlation method[J]. Journal of Traffic and Transportation Engineering, 2020, 20(2): 55–65.

[4] LI Jian, CHEN Shan-xiong, YU Fei, et al. Discussion on mechanism of reinforcing high and steep slope with prestressed anchor cable[J]. Rock and Soil Mechanics, 2020, 41(2): 707–713.

[5] ZHANG Fa-ming, ZHAO Wei-bing, LIU Ning, et al. Long-term performance and load prediction model of prestressed cables[J]. Chinese Journal of Rock Mechanics and Engineering, 2004, 23(1): 39–43.

[6] LI Ying-yong, WANG Meng-shu, ZHANG Ding-li, et al. Study on influential factors and model for variation of anchor cable prestress[J]. Chinese Journal of Rock Mechanics and Engineering, 2008, 27(Suppl.1): 3140–3146.

[7] XIE Can, LI Shu-chen, LI Shu-cai, et al. Study of anchorage force loss of anchor cable under seepage flow and soil creep[J]. Rock and Soil Mechanics, 2017, 38(8): 2313–2321, 2334.

[8] WANG Wei-ming, CAO Zheng-long, WANG Gang-gang, et al. Prestress loss of anchor cables in thick alluvial clay[J]. Chinese Journal of Geotechnical Engineering, 2014, 36(9): 1607–1613.

[9] ZHU Han-ya, SHANG Yue-quan, LU Xi-ming, et al. Coupling analysis of long-term prestress loss and slope creep[J]. Chinese Journal of Geotechnical Engineering, 2005, 27(4): 464–467.

[10] WANG Qing-biao, ZHANG Cong, WANG Hui, et al. Study of coupling effect between anchorage force loss of prestressed anchor cable and rock and soil creep[J]. Rock and Soil Mechanics, 2014, 35(8): 2150–2156, 2162.

[11] CHEN Tuo, CHEN Guo-qing, HUANG Run-qiu, et al. A model of anchorage force loss of anchor cable during high slope strong unloading[J]. Rock and Soil Mechanics, 2018, 39(11): 4125–4132.

[12] WANG Guo-fu, LI Qiang, LU Lin-hai, et al. A coupled model research of anchor prestress loss considering the relaxation characteristics of anchor[J]. Chinese Journal of Underground Space and Engineering, 2017, 13(6): 1585–1591.

[13] XIAO Shi-guo, CAO Shun-li, ZHAO Lin-zhi. Analysis model for relaxation effect of pulling force of prestressed anchor cables used in reinforcing rock mass[J]. Journal of Beijing University of Technology, 2020, 46(8): 940–947.

[14] LU Guang-lu. Experiment study on the stress relaxation in low relaxation prestressing wires[J]. Journal of Shanghai Tiedao University, 1997(2): 46–52.

[15] XU Yi-qing, DENG Shao-yu, GE Qi. Prediction models for short-term and long-term pre-stress loss of anchor cable[J]. Rock and Soil Mechanics, 2020, 41(5): 1663–1669.

[16] CHEN Yuan-jiang, YIN Jin, HU Yi-fu. Research on prestress quantitative loss law of soft rock slope anchor cable[J]. Chinese Journal of Rock Mechanics and Engineering, 2013, 32(8): 1685–1691.

[17] SHEN Jun, GU Jin-cai, ZHANG Xiang-yang, et al. Field pull-out test research on tension and pressure unbounded

anchor cables[J]. Chinese Journal of Rock Mechanics and Engineering, 2012, 31(Suppl.1): 3291–3297.

[18] YANG Qing, ZHU Xun-guo, LUAN Mao-tian. Developmet of hyperbolic model for fully grouting rock bolt and parameters analysis for anchoring effect[J]. Chinese Journal of Rock Mechanics and Engineering, 2007, 26(4): 692–698.

[19] ZHOU Yong-jiang, HE Si-ming, YANG Xue-lian. Study on prestress loss of anchor cables under long-term loading[J]. Rock and Soil Mechanics, 2006, 27(8): 1353–1356.

[20] DONG Zhi-hong, DING Xiu-li, HUANG Shu-ling, et al. Analysis of ageing-stress characteristics and long-term bearing risk of anchor cable for a large cavern in high geo-stress area[J]. Rock and Soil Mechanics, 2019, 40(1): 351–362.

[21] WEI Li-de, XU Wei-ya, YANG Chun-he, et al. Study on elastoplastic constitutive model of rock with statistical damage[J]. Chinese Journal of Rock Mechanics and Engineering, 2004, 23(12): 1971–1975.

[22] CHENG Liang-kui, ZHANG Pei-wen, WANG Fan. Several mechanical concepts for anchored structures in rock and soil[J]. Chinese Journal of Rock Mechanics and Engineering, 2015, 34(4): 668–682.

[23] CHEN An-min, GU Jin-cai, SHEN Jun, et al. Impact of length and prestress value of anchor cable on its reinforcement effect[J]. Chinese Journal of Rock Mechanics and Engineering, 2002, 21(6): 848–852.

[24] YIN Yan-chun, ZHAO Tong-bin, TAN Yun-liang, et al. Research of stress distribution evolution law and influencing factors[J]. Journal of Mining & Safety Engineering, 2013, 30(5): 712–716.

[25] HUANG Ming-hua, ZHOU Zhi, OU Jin-ping. Nonlinear full-range analysis of load transfer in fixed segment of tensile anchors[J]. Chinese Journal of Rock Mechanics and Engineering, 2014, 33(11): 2190–2199.

[26] ZHANG Fa-ming, LIU Ning, CHEN Zu-yu, et al. Analysis of factors affected on load losses of high capacity and long rock anchors[J]. Rock and Soil Mechanics, 2003, 24(2): 194–197.

[27] FU Dan, GUO Hong-xian, CHENG Xiao-hui, et al. Working stress measurement of prestressed anchor cables: detection mechanism and experimental study of lift-off test[J]. Rock and Soil Mechanics, 2012, 33(8): 2247–2252.

[28] RUAN Bo, XIAO Wu-quan. Influence factors of load at lock off of prestressed anchors based on grey relevant degree theory[J]. Journal of Railway Science and Engineering, 2011, 8(3): 38–41.

[29] ZHAO Yan-lin, TANG Jin-zhou, FU Cheng-cheng, et al. Rheological test of separation between viscoelastic-plastic strains and creep damage model[J]. Chinese Journal of Rock Mechanics and Engineering, 2016, 35(7): 1297–1308.

[30] Ministry of Transport of the People's Republic of China. JTG 3362－2018 Specifications for design of highway reinforced concrete and prestressed concrete bridges and culverts[S]. Beijing: China Planning Press, 2018.

[31] Ministry of Housing and Urban-Rural Development of the People's Republic of China. GB50086 － 2015 Technical code for engineering of ground anchorages and shotcrete support[S]. Beijing: China Planning Press, 2015.

[32] LI Yun-peng, WANG Zhi-yin, DING Xiu-li. Model identification for rheological load test curve and its application[J]. Journal of China University of Petroleum (Edition of Natural Science), 2005(2): 73–77.

[33] FENG Zhong-ju, WANG Zheng-bin WANG Fu-chun, et al. A pullout device, pullout detection device and method of anchorage system: CN110057699A[P]. 2019-07-26.